Volume 1 | Number 1 | Jan 2013 | Pages 1–100

ChemComm

Chemical Communications
www.rsc.org/chemcomm

ROYAL SOCIETY OF CHEMISTRY

Journal Name

COMMUNICATION

A universal molecular translator for non-nucleic acid targets that enables dynamic DNA assemblies and logic operations†

Wei Tang, Shichao Hu, Huaming Wang, Yan Zhao, Na Li and Feng Liu*

A universal molecular translator based on the target-triggered DNA strand displacement was developed, which was able to convert various kinds of non-nucleic acid targets into a unique output DNA. This translation strategy was successfully applied in directing dynamic DNA assemblies and in realizing three-input logic gate operations.

Advances made over the past decade in the DNA nanotechnology have facilitated applications of molecular imaging and disease diagnosis both *in vitro* and *in vivo*.[1] A series of dynamic DNA devices, including DNA nanomachines,[2] catalytic circuits,[3] and logic gates,[4] have been rationally constructed, most of which are driven by toehold-mediated DNA strand displacement reactions based on nucleic acid inputs.[5] It is highly desired to use various kinds of non-nucleic acid targets to control the operation of dynamic DNA devices. Thus, the development of molecular translators to translate any designated non-nucleic acid target into a unique output DNA sequence would be extremely beneficial for the rational engineering design of advanced target-fuelled dynamic DNA devices. One general approach to fabricate the molecular translators for small molecules is based on the allosteric activation of the output DNA.[5b,6] First, the output DNA was sequestered by steric and topological constraints or within a duplex, and then activated by allosteric binding of the input with the function strand. Recently, the binding-induced molecular translator was constructed for converting the protein inputs to the output DNA.[7] Binding of the specific protein to affinity ligands on two probes increased the local effective concentrations of the probes, resulting in the release of the output DNA.[8] We previously proposed the DNA tetraplexes-based toehold activation strategy in response to three targets which must bind to two affinity fragments.[9] To date, most molecular translators are designed for a single target or one class of targets, and lack further applications in designing target-fuelled molecular devices.

Herein, we report a facile strategy to construct the molecular translator, which can translate various kinds of non-nucleic acid inputs, such as adenosine triphosphate (ATP), thrombin, Sr^{2+}, and H^+, into a readily detectable output DNA sequence by easily altering the correlative function domain. Additionally, we explore the feasibility for coupling the developed translator with dynamic DNA assemblies, and create three-input AND and OR logic gates through employing this translation strategy, which significantly extend applications of molecular translators in designing target-fuelled molecular devices.
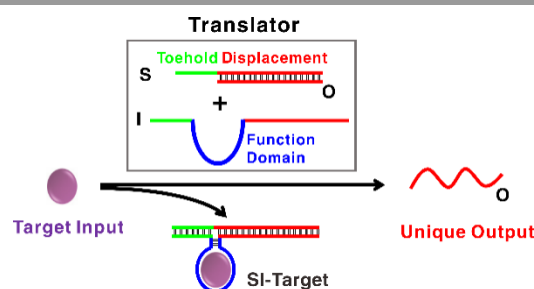
Fig. 1 Principle of the translation strategy. The output DNA **O** hybridizes with **S** to form an **SO** duplex. The invading DNA **I** is designed by inserting a function domain between the toehold and displacement domains. Binding of the target input to the function domain triggers the following strand displacement. Thus, the output DNA **O** is released from **S** by forming a TWJ. The nucleotide sequences of all strands are provided in Table S1–S6 of ESI†.

The molecular translator design is illustrated in Fig. 1. The unique output DNA (**O**) hybridizes with the substrate DNA (**S**) to form an **SO** duplex. An invading DNA (**I**) which contains a function domain inserted between the toehold and displacement domains is designed. The function domain as the target-recognition element can specifically bind with the designated target input. The invading DNA **I** first docks to **S** through hybridization of its toehold domain. In the absence of the target input, the free-state function domain keeps the displacement domain on **I** away from the docking site. Thus, the output DNA **O** can hardly been displaced from **S**. While the target input is present, the target binding triggers the adaptive folding and compaction of the function domain,[10] which brings the displacement domain on **I** in close proximity to the docking site. As a result, the

release of the output DNA **O** is promoted by forming a three-way junction (TWJ) through the strand displacement reaction between **SO** and **I**. The key feature of our strategy is the adaptive folding and compaction of the function domain triggered by target binding, which allows the translator to convert a non-nucleic acid input into a unique output DNA by easily altering the correlative function domain.

To test the feasibility of our strategy, we first constructed a molecular translator for ATP. The ATP binding aptamer was used as the function domain inserted between the toehold and displacement domains on the invading DNA (I_A).[11] The stability of the formed TWJ is considered as one of key elements for the performance of the molecular translator.[12] We designed a series of junctions to investigate the stability of TWJs. The junction parameters are annotated by (x,y,z), where x and y denote the numbers of the bugled adenosines at 3' and 5' of I_A respectively, and z is the number of the extra A-T base pairs (Fig. 2A). The output DNA **O** was labeled by the 5'-TET and the 3'-TAMRA, serving as the signal reporter (Text S2, ESI†). We measured fluorescence signals of the translator with different junctions in the absence or presence of ATP, and calculated the ratios (k/k_0) of corresponding reaction rate constants (Fig. 2B). A highest ratio is observed for the translator with the junction parameters (2,0,0), indicating which presents the largest signal discrimination in translating the ATP input into the output DNA. So this TWJ with the junction parameters (2,0,0) was carried forward for further studies.
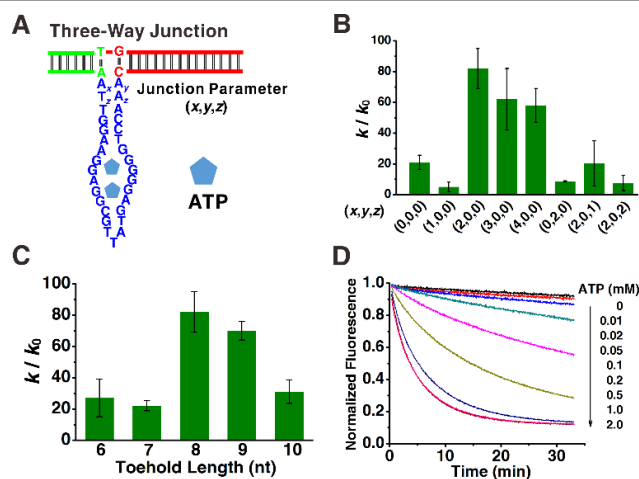

Fig. 2 Molecular translator for ATP. (A) Schematic of the TWJ with the designed junction parameters. Effect of the junction parameters (B) and the toehold lengths (C) on the ratio of reaction rate constants (k/k_0). k_0 and k denote the reaction rate constants in the absence or presence of ATP respectively (Text S2, ESI†). Initial concentrations: 20 nM **SO**, 100 nM I_A, and 2 mM ATP. Error bars represent the standard deviation of three measurements. (D) Effect of ATP concentrations on the translation kinetics. In a typical experiment, the **SO** duplex (1 mL, 20 nM) was placed in a cuvette, and then both I_A (5 μL, 20 μM) and ATP (2 μL at the proper concentration) were added and mixed quickly within 30 s to initiate the reaction. The normalized fluorescence is processed as Text S2 of ESI†.

The toehold length is another important factor in designing the molecular translator. Changing the toehold lengths from 6 nt to 10 nt, the largest translation discrimination of the translator is shown for 8 nt length toehold (Fig. 2C). We also assessed the behavior of the translator to convert the ATP input to the output DNA by varying ATP concentrations. As shown in Fig. 2D, the translation rates can be accelerated in an ATP concentration-dependent way. And the

fluorescence intensities are proportional to the concentration of ATP in the range from 10 to 500 μM. Meanwhile, the ATP input with minimum concentration of 10 μM can be applied to effect the translation, which is an obvious improvement compared with the reported ATP translators.[5b,6a] This translator also shows a higher selectivity for ATP than that of TTP, CTP, and GTP (Fig. S1, ESI†). Therefore, we demonstrated the feasibility of translating a designed small molecule input into a desired sequence-specific output DNA by the constructed molecular translator.
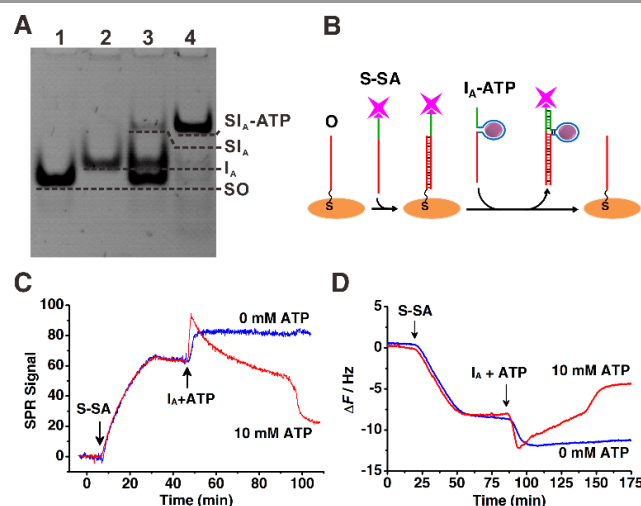

Fig. 3 Validation of the translation mechanism for ATP. (A) Native PAGE (12%) analysis. Lane 1: 1 μM **SO**, lane 2: 1 μM I_A, lane 3: 1 μM **SO** and 1 μM I_A, lane 4: 1 μM **SO**, 1 μM I_A, and 1 mM ATP. (B) Rationale of the real time evaluations by SPR and QCM. Real time monitoring of the translation processes by SPR (C) and QCM (D). First, a 100 nM **S-SA** mixture was injected to hybridize with **O**, and then solutions contained 0.5 μM I_A for QCM (1 μM I_A for SPR) in the absence or presence of 10 mM ATP were injected respectively.

In order to verify whether the proposed translation reaction proceeded as designed, the native polyacrylamide gel electrophoresis (PAGE) experiment was carried out (Fig. 3A). In the absence of the ATP input (lane 3), strong bands of **SO** and I_A are observed, and the band of SI_A is almost invisible, indicating that the translation reaction is extremely slow. However, in the presence of the ATP input (lane 4), the bands of **SO** and I_A are nearly disappeared, and the strong band of SI_A-ATP is observed, which proves the formation of the three-way junction complex with the release of the output DNA **O**. The surface plasmon resonance (SPR) and the quartz crystal microbalance (QCM) are relatively new and powerful tools for real-time monitoring intermolecular interactions. Furthermore, the target-triggered strand displacement process was monitored by using SPR and QCM respectively (Fig. 3B). The output DNA **O** was first immobilized on the chip surface. Then streptavidin (**SA**) labeled substrate DNA (**S-SA**) hybridized with **O** to produce a sharp signal shift due to the signal amplification of streptavidin (Fig. 3C and 3D). After only injecting I_A, the SPR signal increased and the QCM frequency decreased, which were resulted by the hybridization of **S-SA** and I_A at the toehold domain. However, injecting I_A mixed with ATP, I_A-ATP first docked to **S-SA** through hybridization of its toehold domain. Subsequently, SPR and QCM signals decreased and increased respectively, exhibiting that I_A-ATP hybridized with **S-SA** through the strand displacement,

and **S-SA** was released from **O**. These experiment results confirm the rationality of the proposed translation strategy.

To confirm the generality of our strategy, we designed three molecular translators for other non-nucleic acid targets, including thrombin, Sr^{2+}, and H^+ by easily altering the function domain on I, respectively. The thrombin binding aptamer (Fig. S2, ESI†), the G-rich sequence responding to Sr^{2+}(Fig. S3, ESI†), and the C-rich sequence responding to H^+ (Fig. S4, ESI†) were used as the function domains inserted between the toehold and displacement domains on **I**, respectively. Binding of the target input to the correlative function domain triggers the following strand displacement, resulting in the release of the output DNA **O** by forming TWJ. Similarly, to achieve the best performance of the designed molecular translators, we optimized the junction parameters (x,y,z) of TWJs and the toehold lengths in each translator (Fig. S5–S10, ESI†) respectively. The behaviors of the translators were assessed by varying input concentrations. Using the optimal designs, the translators show dose-responses to the thrombin input in the range from 2 to 100 nM (Fig. S11, ESI†), the Sr^{2+} input in the range from 0.2 to 30 mM (Fig. S12, ESI†), and the pH input in the range from 6.2 to 5.0 (Fig. S13, ESI†), respectively. The translators also show a higher selectivity for thrombin (Fig. S14, ESI†) and Sr^{2+} (Fig. S15, ESI†), respectively. Meanwhile, PAGE experiments confirmed the rationality of the constructed translators (Fig. S16–S18, ESI†). Therefore, with this facile translation strategy, various kind of non-nucleic acid targets such as small molecules, proteins, metal ions, and H^+ can be successfully converted into a unique output DNA sequence.
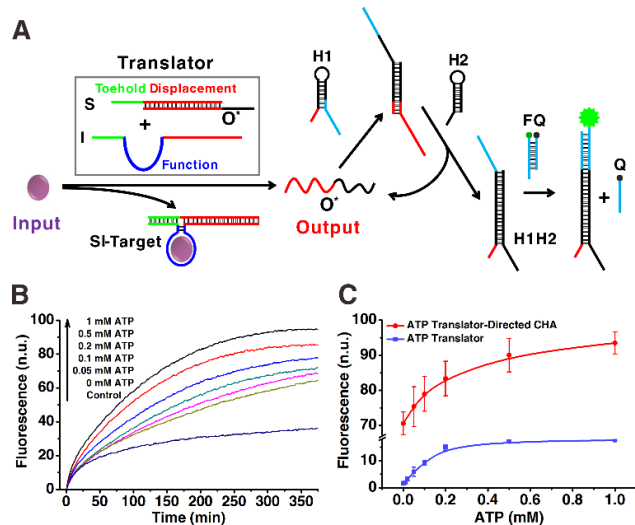

Fig. 4 (A) Principle of the translator-directed CHA. (B) Estimation of the translator-directed CHA. The test solutions contained 20 nM **SO***, 50 nM **I$_A$**, 100 nM **H1**, 500 nM **H2**, 100 nM **FQ**, and varying ATP concentrations. Control test solution contained 100 nM **H1**, 500 nM **H2** and 100 nM **FQ**. The fluorescence intensity was normalized such that 1 normalized unit (n.u.) corresponds to the fluorescence intensity of 1 nM fluorophore-labeled strand. (C) Increases in fluorescence intensity as a function of ATP concentrations. Error bars represent the standard deviation of three measurements.

To demonstrate the ability of our strategy to control the operation of dynamic DNA assemblies, we applied the molecular translator to direct the catalyzed hairpin assembly (CHA)[3a,6a] and the hybridization chain reaction (HCR)[3b]. Take ATP for example, the principle of the

translator-directed CHA is shown in Fig. 4A. Hairpins (**H1** and **H2**) can potentially hybridize to each other. However, the spontaneous hybridization between **H1** and **H2** is kinetically hindered by occluding complementary regions within intramolecular hairpin secondary structures. The output DNA **O*** is designed as the initiator of CHA and sequestered in the complementary part of **SO***. While the target is added, the released output DNA **O*** from **S** hybridizes with **H1** to open the hairpin structure through the strand displacement. The newly exposed sticky end of **H1** again initiates a strand displacement with **H2** to release **O***. Thus, **O*** clearly plays a role as a catalyst to trigger the hybridization of additional pairs of **H1** and **H2**. To monitor the assembly of **H1** and **H2**, a fluorescent reporter was designed by hybridizing a FAM-labeled strand (**F**) and a Dabcyl-labeled strand (**Q**). The fluorescence of **F** is efficiently quenched by the hybridized **Q**. One sticky end of **H1** on the **H1H2** complex can hybridize with **F** to release **Q**, leading to an increase in the fluorescent intensity.

Coupling the translator to CHA, we monitored the fluorescence intensity increases as a function of time (Fig. 4B), a dose-dependent response to the ATP input is observed. The fluorescence signal has also been amplified by over 5-fold throughout the concentration range of 10 μM to 1 mM, comparing with that detected by the ATP translator, which provides an amplified response of the ATP concentration (Fig. 4C). The results demonstrated the ability of the developed translation strategy to direct the catalyzed hairpin assembly.

We also designed a translator-directed HCR (Fig. S19, ESI†). Two complementary hairpins (**H3** and **H4**) are stable at room temperature, since each hairpin is caught in a kinetic trap. The output DNA **O*** is designed as the initiator of HCR and sequestered in the complementary part of **SO***. While the target is added, the released output DNA **O*** triggers a chain reaction of alternating kinetic escapes by the two hairpin species corresponding to "polymerization" into an elongated double helix. Agarose gel electrophoresis was applied to demonstrate the growth of the double helix. The average molecular weight of resulting products is inversely related to ATP concentrations (Fig. S20, ESI†), suggesting the ability of this translation strategy to direct HCR. The results of the translator-directed CHA and HCR demonstrated the feasibility of controlling dynamic DNA assemblies by non-nucleic acid targets.

DNA is a powerful and versatile nanoscale material for constructing complex molecular circuits, where the basic building blocks are logic gates. We created DNA logic gates, using various non-nucleic acid targets as inputs by employing the proposed translation strategy. As shown in Fig. 5A, the three-input AND gate consists of a gate complex assembled by an output DNA and three gate DNAs (**S$_x$**, **S$_y$**, and **S$_z$**), and three invading DNAs (**I$_x$**, **I$_y$**, and **I$_z$**) including function domains for thrombin, Sr^{2+}, and ATP, respectively. Each gate strand can hybridize with its corresponding invading DNA. When the first thrombin input is present, the target binding triggers the strand displacement reaction, resulting in the release of the first gate DNA **S$_x$**. The toehold for the subsequent invading DNA **I$_y$** is exposed. Similar processes can occur for the second Sr^{2+} input and the following third ATP input. The output DNA **O** labeled by the 5'-TET and the 3'-TAMRA is released only if all of three inputs are present. The three-input AND gate has eight entries in its truth table and was tested by fluorescence experiments. When the three inputs were present at the same time,

an efficient fluorescence decrease was observed by the release of **O**, demonstrating a three-input AND gate device.
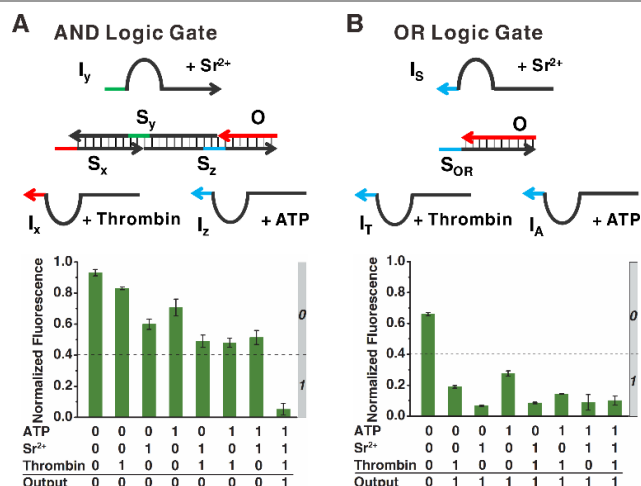

Fig. 5 Simplified schematics of three-input AND and OR gates (top), and the experimentally observed fluorescence outputs from execution of each simple circuit with every combination of inputs (bottom). Experiments were conducted with gate concentrations of 50 nM, invading DNA concentrations of 100 nM, and input concentrations of 0.1 μM, 10 mM, and 2 mM for thrombin, Sr^{2+}, and ATP, respectively. Error bars represent the standard deviation of three measurements.

A three-input OR gate was also designed (Fig. 5B). The gate complex is assembled by the output DNA **O** and one gate DNA (**S_OR**). The three invading DNAs (**I_T**, **I_S**, and **I_A**) designed have the same toehold and displacement domains, all of which are complementary to **S_OR**, respectively. Thus, the output will be true if any of the inputs is true. We tested the output of the eight entries in the truth table. Only when none of the three inputs were present, the fluorescence of **O** would be maintained. Therefore, utilizing our strategy, we successfully realized three-input AND and OR logic gate operations with various non-nucleic acid targets as inputs.

In conclusion, we have successfully constructed the translator for various non-nucleic acids by utilizing the target-triggered DNA strand displacement. The non-nucleic acid targets, such as ATP, thrombin, Sr^{2+}, and H^+, can be translated into a unique output DNA sequence by easily altering the function domain respectively. Thus, our strategy should be easily applicable to other non-nucleic acid targets which can trigger the folding and compaction of their binding sequences. In particular, we have demonstrated that the designed translator is able to direct CHA and HCR, possessing the feasibility of controlling the operation of dynamic DNA devices. We also have realized three-input AND and OR logic gate operations by applying this strategy, which convincingly provides a new route for designing DNA-based logic circuits. Potential applications of our strategy in designing target-fuelled molecular devices may open new possibilities in molecular imaging, disease diagnosis, and even logic processing both *in vitro* and *in vivo*.

Notes and references

Beijing National Laboratory for Molecular Sciences, Key Laboratory of Bioorganic Chemistry and Molecular Engineering of Ministry of Education, College of Chemistry and Molecular Engineering, Peking University, Beijing 100871, China. E-mail: liufeng@pku.edu.cn.
† Electronic Supplementary Information (ESI) available: Detailed experimental methods and additional data. See DOI: 10.1039/c000000x/

1 (*a*) E. Stulz, G. Clever, M. Shionoya and C. Mao, *Chem. Soc. Rev.*, 2011, **40**, 5633; (*b*) Y. Tian, Y. He, Y. Chen, P. Yin and C. Mao, *Angew. Chem. Int. Ed.*, 2005, **44**, 4355; (*c*) S. Venkataraman, R. M. Dirks, C. T. Ueda and N. A. Pierce, *Proc. Natl. Acad. Sci. U.S.A.*, 2010, **107**, 16777; (*d*) X. Liu, H. Yan, Y. Liu and Y. Chang, *Small*, 2011, **7**, 1673; (*e*) J. Hemphill and A. Deiters, *J. Am. Chem. Soc.*, 2013, **135**, 10512; (*f*) S. Modi, M. G. Swetha, D. Goswami, G. D. Gupta, S. Mayor and Y. Krishnan, *Nat. Nanotechnol.*, 2009, **4**, 325.

2 (*a*) J. Bath and A. J. Turberfield, *Nat. Nanotechnol.*, 2007, **2**, 275; (*b*) T. Omabegho, R. Sha and N. C. Seeman, *Science*, 2009, **324**, 67; (*c*) Y. Chen, S. H. Lee and C. Mao, *Angew. Chem. Int. Ed.*, 2004, **43**, 5335; (*d*) H. Liu and D. Liu, *Chem. Commun.*, 2009, 2625.

3 (*a*) P. Yin, H. M. T. Choi, C. R. Calvert and N. A. Pierce, *Nature*, 2008, **451**, 318; (*b*) R. M. Dirks and N. A. Pierce, *Proc. Natl. Acad. Sci. U.S.A.*, 2004, **101**, 15275; (*c*) G. Seelig, B. Yurke and E. Winfree, *J. Am. Chem. Soc.*, 2006, **128**, 12211; (*d*) D. Y. Zhang, A. J. Turberfield, B. Yurke and E. Winfree, *Science*, 2007, **318**, 1121; (*e*) Y. S. Jiang, S. Bhadra, B. Li and A. D. Ellington, *Angew. Chem. Int. Ed.*, 2014, **53**, 1845; (*f*) X. Chen, Y. H. Lin, J. Li, L. S. Lin, G. N. Chen, H. H. Yang, *Chem. Commun.*, 2011, **47**, 12116.

4 (*a*) G. Seelig, D. Soloveichik, D. Y. Zhang and E. Winfree, *Science*, 2006, **314**, 1585; (*b*) L. Qian and E. Winfree, *Science*, 2011, **332**, 1196; (*c*) J. Zhu, L. Zhang, Z. Zhou, S. Dong and E. Wang, *Chem. Commun.*, 2014, **50**, 3321; (*d*) W. Li, Y. Yang, H. Yan and Y. Liu, *Nano Lett.*, 2013, **13**, 2980.

5 (*a*) B. Yurke and A. P. Mills, *Genet. Program. Evol. Mach.*, 2003, **4**, 111; (*b*) J. M. Picuri, B. M. Frezza and M. R. Ghadiri, *J. Am. Chem. Soc.*, 2009, **131**, 9368; (*c*) A. J. Genot, D. Y. Zhang, J. Bath and A. J. Turberfield, *J. Am. Chem. Soc.*, 2011, **133**, 2177.

6 (*a*) B. Li, A. D. Ellington and X. Chen, *Nucleic Acids Res.*, 2011, **39**, e110; (*b*) Y. Xing, Z. Yang and D. Liu, *Angew. Chem. Int. Ed.*, 2011, **50**, 11934; (*c*) R. A. Muscat, J. Bath and A. J. Turberfield, *Small*, 2012, **8**, 3593.

7 (*a*) F. Li, H. Zhang, C. Lai, X. F. Li and X. C. Le, *Angew. Chem. Int. Ed.*, 2012, **51**, 9317; (*b*) F. Li, H. Zhang, Z. Wang, X. Li, X. F. Li and X. C. Le, *J. Am. Chem. Soc.*, 2013, **135**, 2443; (*c*) F. Li, Y. Lin and X. C. Le, *Anal. Chem.*, 2013, **85**, 10835.

8 H. Zhang, F. Li, B. Dever, C. Wang, X. F. Li and X. C. Le, *Angew. Chem. Int. Ed.*, 2013, **52**, 10698.

9 W. Tang, H. Wang, D. Wang, Y. Zhao, N. Li and F. Liu, *J. Am. Chem. Soc.*, 2013, **135**, 13628.

10 (*a*) R. P. Fahlman and D. Sen, *J. Am. Chem. Soc.*, 2002, **124**, 4610; (*b*) Y. C. Huang, B. Ge, D. Sen and H. Z. Yu, *J. Am. Chem. Soc.*, 2008, **130**, 8023; (*c*) J. M. Thomas, H. Z. Yu and D. Sen, *J. Am. Chem. Soc.*, 2012, **134**, 13738; (*d*) J. M. Thomas, B. Chakraborty, D. Sen and H. Z. Yu, *J. Am. Chem. Soc.*, 2012, **134**, 13823.

11 D. E. Huizenga and J. W. Szostak, *Biochemistry*, 1995, **34**, 656.

12 (*a*) J. B. Welch, F. Walter and D. M. J. Lilley, *J. Mol. Biol.*, 1995, **251**, 507; (*b*) C. G. Sankar and D. Sen, *J. Mol. Biol.*, 2004, **340**, 459.